Forensic Science, Medicine, and Pathology

ISSN 1547-769X/06/2:115–126/$30.00 (Online) 1556-2891
DOI: 10.1385/Forensic Sci. Med. Pathol.:2:2:115

ORIGINAL ARTICLE

Neuropathological Alterations in Drug Abusers

*The Involvement of Neurons, Glial, and Vascular Systems**

Andreas Büttner[1] *and Serge Weis*[2]

[1]Institute of Legal Medicine, Ludwig-Maximilians University, Munich, Germany; and [2]Stanley Laboratory of Brain Research and Neuropathology, The Stanley Medical Research Institute, Departments of Psychiatry and Pathology, Uniformed Services University of the Health Sciences, Bethesda, MD

Address for correspondence and reprints:

Dr. Andreas Büttner
Institute of Legal Medicine,
Ludwig-Maximilians University,
Munich, Germany
Frauenlobstr. 7a
E-mail: Andreas.Buettner@med.uni-muenchen.de

Accepted for publication:
February 20, 2006

Abstract

Because the effects of drug abuse on the cellular elements of the human brain have not been studied systematically, an investigation was performed using histology, immunohistochemistry, and morphometry. The main cortical and subcortical brain areas of 50 polydrug deaths were analyzed as compared with controls.

In the brains of drug abusers, a significant neuronal loss was present. Interestingly, the number of glial fibrillary acidic protein (GFAP)-positive astrocytes was reduced. The numerical density of perivascular and parenchymal microglia was increased in the white matter and in most subcortical regions. In the white matter there were widespread ß-amyloid precursor protein deposits. Furthermore, there was a prominent vascular hyalinosis, endothelial cell proliferation, and a loss of immunoreactivity for collagen type IV within the vascular basal lamina.

The neuronal loss seems to be the result of a direct impairment of nerve cells and, indirectly, to a damage of astrocytes, axons, and the microvasculature. The reduction of GFAP-positive astrocytes is also indicative of a drug-induced damage. The axonal injury suggests a toxic-metabolic drug effect, whereas the concomitant activation of microglia is indicative of a long-standing progressive process. The noninflammatory vasculopathy can be considered as the morphological substrate of a disturbed blood–brain barrier. Our findings demonstrate that drugs of abuse initiate a cascade of interacting toxic, vascular, and hypoxic factors that finally result in widespread disturbances within the complex network of central nervous system cell–cell interactions.

Key Words: Forensic neuropathology; drug abuse; neuropathology; astrocytes; microglia; microvessels.

(DOI: 10.1385/Forensic Sci. Med. Pathol.:2:2:1)

INTRODUCTION

Drug abuse represents a significant forensic issue worldwide. Although no brain lesion specific for drug abuse exists, a broad spectrum of changes affecting the central nervous system (CNS) is seen in drug abusers *(1,2)*. In addition, morphological, physiological, and neurochemical abnormalities have been demonstrated by using neuroradiological techniques such as computed tomography, magnetic resonance imaging, magnetic resonance spectroscopy, positron emission tomography, or single photon emission computed tomography*(1,3)*.

However, because the consequences of drug abuse on the cellular elements of the brain have not been studied systematically, an investigation was performed using histology, immunohistochemistry, and morphometry. The analysis included the spectrum, frequency, and topography of histopathological alterations in the brains of polydrug abusers as compared with controls through the determination of nerve cell density, the reaction pattern of astrocytes and microglia, as well as an examination of the white matter and the cerebral microvasculature.

*This study was presented at the Sixth International Symposium in Advanced Legal Medicine (ISLAM), Hamburg, Germany, September 2006.

MATERIAL AND METHODS

Brain specimens of 50 polydrug abusers and 30 controls (subjects with no history of polydrug abuse) were examined (Tables 1, 2). Autopsy included macroscopic and histological examination of all major organs (Table 3). The police records were used to obtain information regarding history of CNS trauma, circumstances of death, and the estimated duration of drug abuse. The age of the 36 male polydrug abusers ranged from 16 to 44 years (mean age: 26 years), and that of the 14 female polydrug abusers ranged from 17 to 41 years (mean age: 25 years). The age of the 20 male controls ranged from 24 to 57 years (mean age: 41 years) and that of the 10 female controls ranged from 16 to 60 years (mean age: 37 years). The age difference between both groups was chosen intentionally to compare the findings in the polydrug abusers with possible age-dependent CNS alterations. There was no significant difference in the postmortem interval between both groups. All persons tested negative for HIV-1 infection. In all cases, toxicological analyses were performed on blood, urine, and gastric content. In addition, blood alcohol concentrations were measured in every case. All the control cases tested negative for illicit drugs and alcohol.

At autopsy, brain weight, signs of brain edema, and signs of raised intracranial pressure were noted. The brains were fixed for 2 weeks in a 4% phosphate-buffered saline (PBS)-formalin solution. After fixation, the brains were cut in coronal sections. Blocks of the following regions were removed from every case: (1) the orbitofrontal cortex (orb-co) and white matter (orb-wm), (2) the frontal cortex (fro-co) and white matter (fro-wm), (3) the temporal cortex (tem-co) and white matter (tem-wm) including the hippocampal formation (CA1, CA4, granular layer of the dentate gyrus), (4) the parietal cortex (par-co) and white matter (par-wm), (5) the occipital cortex (occ-co) and white matter (occ-wm), (6) the basal ganglia (bggl = caudate nucleus, putamen, globus pallidus) with the internal capsule (caint), (7) the thalamus (thal), (8) the mesencephalon (mes) including the substantia nigra, (9) the pons, (10) the medulla oblongata (med) including the olivary nucleus (olive), and (11) the cerebellum (cer-co, cer-wm) including the dentate nucleus (dent). The specimens were washed in running water, dehydrated, and embedded in paraffin.

Sections were cut (5 µm) and histological examination encompassed the hematoxylin and eosin (H&E), cresyl-violet (Nissl stain), Luxol-Fast-Blue (LFB), van-Gieson Elastica, Periodic Acid-Schiff (PAS), and Prussian Blue staining methods. All sections were analyzed systematically for the following criteria: leptomeninges (fibrosis, congestion, cell infiltrates), brain edema, vascular congestion, neurons (hypoxic changes, density), white matter damage, presence of gliomesenchymal nodules, and vascular system (morphology of blood vessels, perivascular cuffing, perivascular hemorrhages).

Deparaffinized 5-µm-thick sections were immunostained with the avidin-biotin-complex (ABC) method. For labeling astrocytes, a monoclonal antibody (MAb) against glial fibrillary acidic protein (GFAP, dilution 1:100, DAKO, Germany) was used and for microglia, an MAb against the human lymphocyte antigens (HLA)-DP, DQ, DR antigen (CR 3/43, dilution 1:100, DAKO, Germany, predigestion with formic acid) was used. The vascular basal lamina was immunostained with an MAb against collagen type IV (dilution 1:200, DAKO, Germany, predigestion with protease). For the investigation of white matter changes, an MAb against ß-amyloid precursor protein (ß-APP 695a, dilution 1:200, Zytomed, Germany, microwave antigen-retrieval procedure with citrate buffer) was used. The antigens were detected with a Histostain®-Plus Peroxidase Kit (Zytomed, Germany).

The neurohistopathological analyses were performed using a semiquantitative scoring system with 0 being not present; 1, moderately present; and 2, strongly present.

Table 1
Data for the Control Cases

Case no.	*Age/ gender*	*Brain weight (g)*	*Cause of death*
C01	12/F	1296	Homicide, stabbing
C02	16/F	1330	Hanging
C03	24/F	1510	Homicide, stabbing
C04	24/M	1370	Myocarditis
C05	27/M	1478	Hanging
C06	28/F	1290	Ovarian carcinoma
C07	30/M	1716	Hanging
C08	32/M	1655	Hanging
C09	33/M	1606	Hanging
C10	35/F	1445	Amniotic fluid embolism
C11	35/M	1220	Cardiomyopathy
C12	38/M	1530	Esophageal carcinoma
C13	38/M	1379	Myocardial infarction
C14	39/F	1410	Breast carcinoma
C15	39/M	1400	Hemorrhagic shock
C16	40/M	1643	Hanging
C17	42/M	1521	Hanging
C18	43/M	1350	Pneumonia
C19	44/M	1350	Sepsis
C20	45/F	1490	Myocardial infarction
C21	47/M	1521	Hanging
C22	50/M	1210	Myocardial infarction
C23	51/M	1470	Aortic dissection
C24	51/M	1340	Epipharynx carcinoma
C25	51/M	1370	Cardiomyopathy
C26	52/F	1300	Breast carcinoma
C27	55/M	1150	Myocardial infarction
C28	57/M	1360	Pulmonary carcinoma
C29	59/F	1115	Pulmonary artery embolism
C30	60/F	1250	Pneumonia

M, male; F, female.

Table 2
Data for the Drug Fatalities

Case no.	*Age/ gender*	*Brain weight (g)*	*Types of drugs used*	*BAC*	*Duration of drug abuse*
1	16/M	1652	Heroin, dihydrocodeine, benzodiazepines	0,00	9 months
2	16/M	1730	Heroin, dihydrocodeine, benzodiazepines	0,00	NA
3	17/F	1524	Heroin, dihydrocodeine, benzodiazepines	0,00	48 months
4	18/F	1078	Heroin, benzodiazepines	0,00	24 months
5	18/F	1440	MDMA, cannabis	0,59	NA
6	19/M	1744	Heroin, dihydrocodeine, benzodiazepines	0,00	20 months
7	19/M	1422	Heroin, benzodiazepines, cannabis	0,00	10 months
8	19/F	1506	Methadone, cannabis	0,00	NA
9	20/M	1560	Dihydrocodeine, heroin, benzodiazepines, cannabis	1,71	50 months
10	21/M	1187	Dihydrocodeine, heroin, benzodiazepines	0,00	60 months
11	21/M	NA	Dihydrocodeine, heroin, benzodiazepines	0,68	36 months
12	21/M	1452	Heroin, dihydrocodeine,methamphetamine, doxepine	0,00	84 months
13	21/F	1216	Heroin, dihydrocodeine, benzodiazepines	2,07	NA
14	22/M	1521	Heroin, benzodiazepines	0,00	24 months
15	23/M	1659	Methadone, dihydrocodeine, benzodiazepines, cannabis	0,00	33 months
16	23/F	1258	Methadone, cocaine,benzodiazepines,dihydrocodeine	0,00	33 months
17	23/F	1290	Dihydrocodeine, benzodiazepines	0,00	56 months
18	24/M	1532	Heroin, benzodiazepines, cannabis	0,84	NA
19	24/M	1530	Heroin, cocaine, benzodiazepines	1,66	18 months
20	24/M	1549	Heroin, dihydrocodeine, benzodiazepines	0,46	29 months
21	24/M	1359	Cocaine, methamphetamine	0,00	NA
22	24/F	1290	Dihydrocodeine, benzodiazepines, carbamazepin	0,00	23 months
23	24/F	1236	Dihydrocodeine, trimipramine, imipramine	0,00	20 months
24	25/M	1348	Heroin, dihydrocodeine, cocaine	0,00	76 months
25	26/M	1495	Heroin, benzodiazepines	0,00	60 months
26	26/M	1456	Heroin, dihydrocodeine, benzodiazepines, cannabis	0,00	108 months
27	26/F	1450	Heroin, dihydrocodeine, benzodiazepines	0,00	110 months
28	27/M	1450	Dihydrocodeine, heroin, benzodiazepines	0,00	24 months
29	28/M	1659	Heroin, dihydrocodeine, benzodiazepines	0,00	53 months
30	28/F	1307	Methadone, heroin, dihydrocodeine	0,00	60 months
31	29/M	1547	Dihydrocodeine, benzodiazepines, cannabis	0,57	NA
32	29/M	1567	Methadone, benzodiazepines, cannabis	0,00	41 months
33	30/M	1579	Dihydrocodeine, benzodiazepines	0,00	141 months
34	30/M	1493	Dihydrocodeine, cocaine, benzodiazepines, doxepine	0,00	133 months
35	31/M	1453	Cocaine, cannabis	0,00	4 months
36	31/M	1499	Heroin, dihydrocodeine, benzodiazepines	0,00	108 months
37	31/M	1591	Heroin, benzodiazepines	0,00	121 months
38	31/W	1324	Dihydrocodeine, codeine, cocaine, benzodiazepines	0,00	120 months
39	32/M	1282	Dihydrocodeine, methadone, trimipramine	1,14	168 months
40	33/M	1462	Heroin, dihydrocodeine, benzodiazepines	0,00	145 months
41	33/M	NA	Heroin, MDMA, amphetamine, benzodiazepines	0,04	59 months
42	34/M	1345	Heroin, benzodiazepines	1,71	NA
43	34/M	1585	Methadone, benzodiazepines	0,00	107 months
44	36/M	1740	Heroin, cocaine, benzodiazepines	0,00	36 months
45	37/M	1525	Heroin, benzodiazepines	0,65	26 months
46	38/F	1396	Cocaine, methadone, benzodiazepines	0,00	264 months
47	39/M	1383	Dihydrocodeine, benzodiazepines	0,27	174 months
48	40/M	1611	Dihydrocodeine, codeine, heroin	0,00	110 months
49	41/W	1354	Codeine, benzodiazepines, carbamazepine	0,72	NA
50	44/M	1556	Heroin, dihydrocodeine, benzodiazepines	0,54	197 months

NA, data not available.

Table 3
Major Findings of the Peripheral Organs of the Drug Fatalities

Case no.	*Skin*	*Heart (g)*	*Lungs (g)*	*Liver (g)*	*Lymph nodes*	*Spleen (g)*	*Thymus (g)*	*Urine (mL)*
1	i.m.	390	R 686, L 580, co	1821, co	pl	215	26	350
2	-	319	R 668, L 626, ed, co, Fe+	1477	-	176	54	250
3	i.m.	268	R 743, L 640, mu, ed, co, Fe+	1696, co	++, pl	137	47	150
4	multiple i.m.	224	R 490, L 249, ed, co	1182, fl	++, pl	703	18	30
5	multiple i.m.	308	R 507, L 514, co	1565, hep	++, pl	192	-	0
6	i.m. & tracks	326	R 767, L 597, co, Fe+	1963, co	++, pl	589	47	700
7	-	302	R 1017, L 869, ed, co, asp	1730, fl	++, pl	197	28	800
8	-	325	R 501, L 460, co	1465, co	++, pl	96	29	10
9	i.m. & tracks	400, hy	R 700, L 616, ed, co, Fe+	1878, co	++, pl	245	65	270
10	multiple i.m.	295	R 950, L 1005, co, Fe+	1276	++, pl	288	44	400
11	i.m. & tracks	358	R 708, L 710, mu, ed, co, Fe+	1582, co	++	167	30	300
12	multiple i.m.	307	R 777, L 709, co, asp, Fe+	1373	++, pl	206	40	550
13	multiple i.m.	286	R 624, L 572, mu, ed, Fe+	1614, co	++, pl	176	32	180
14	fresh i.m.	414, hy	R 917, L 769, mu, ed, co	2156, co	++, pl	209	57	350
15	i.m. & tracks	344	R 638, L 637, co, asp, Fe+	1524, hep	++, pl	133	28	700
16	multiple i.m.	275 fib	R 630, L 502, co, pneumo, Fe+	1393, hep	++	199	25	100
17	i.m. & tracks	278	R 1384, L 1150, ed, Fe+ pneumo	2111, co, hep	++	269	-	10
18	multiple i.m.	541, hy	R 760, L 700, asp, Fe+	3535, fl	++, pl	360	31	100
19	i.m. & tracks	296	R 764, L 778, ed, co, asp	1680	++, pl	118	-	800
20	i.m. & tracks	331	R 723, L 696, ed, co, Fe+	2340, co, hep	++, pl	322	41	400
21	-	379, hy, cb	R 774, L 431, asp, Fe+	1722	-	193	-	180
22	i.m. & tracks	248	R 604, L 645, ed, co, Fe+	1303	++	223	20	350
23	multiple i.m.	240	R 555, L 460, ed, asp, Fe+	1370, hep	++	143	36	0
24	i.m. & tracks	245	R 502, L 594, ed, co, asp, Fe+	1804, co	pl	265	-	250
25	-	408, hy	R 1051, L 895, co	1683, fl, hep	++, pl	170	43	250
26	i.m. & tracks	406, hy	R 594, L 763, ed, co, Fe+	3267, fl, hep	++, pl	515	50	5
27	i.m. & tracks	326 abscesses	R 800, L 750, ARDS, Fe+	1785, necrosis	pl	354	-	4
28	multiple i.m.	365	R 789, L 669, ed, co	1952	++, pl	273	48	300
29	multiple i.m.	458, hy	R 1046, L 783, asp, Fe+	1857, fl	pl	181	35	200
30	fresh i.m.	241	R 860, L 575, mu, ed, co	1130, co	pl	129	39	630
31	multiple i.m.	348	R 320, L 324, co, Fe+	2414, fl	pl	174	-	140
32	i.m. & tracks	349	R 648, L 930, ed, Fe+	1726, co	++, pl	108	27	5
33	multiple i.m.	408, hy	R 856, L 815, co	2669, co	++, pl	505	35	250
34	i.m. & tracks	388	R 706, L 512, ed, co, Fe+	2070, co	++, pl	315	36	700
35	fresh i.m.	536, hy, cb, fib	R 765, L 650, Fe+	2532, co	++	189	-	320
36	i.m. & tracks	504, hy, fib	R 1162, L 960, ed, co, asp, Fe+	2496, co	++, pl	351	96	1
37	i.m. & tracks	460, hy, fib	R 686, L 501, ed, co, asp, Fe+	2252, hep	++, pl	692	73	390
38	i.m. & tracks	299	R 629, L 672, ed, co	1652, co	pl	210	27	150
39	fresh i.m.	323, fib	R 796, L 594, co, asp	1626	++, pl	219	18	400
40	multiple i.m.	336, fib	R 634, L 783, asp, Fe+	1852, co, hep	pl	282	26	200
41	multiple i.m.	349	R 835, L 730, co, Fe+	1865	++	190	-	500
42	multiple i.m.	413, healed endocarditis	R 787, L 823, ed, Fe+	3660, fl	++, pl	260	35	100
43	multiple i.m.	360	R 936, L 769, ed, co, asp, Fe+	2120, co	++	360	41	100
44	i.m. & tracks, abcesses	428, hy	R 830, L 851, ed, co, Fe+	1954, co	++	331	44	300

(Continued)

Table 3 *(Continued)*

Case no.	*Skin*	*Heart (g)*	*Lungs (g)*	*Liver (g)*	*Lymph nodes*	*Spleen (g)*	*Thymus (g)*	*Urine (mL)*
45	i.m. & tracks	326	R 695, L 558, co, Fe+	1823	++, pl	214	20	50
46	i.m. & tracks	257	R 447, L 419, co, Fe+	1540, co	++, pl	123	22	5
47	i.m. & tracks	399, hy, fib	R 677, L 680, ed, Fe+	1966, hep	++, pl	132	43	100
48	i.m. & tracks	378	R 753, L 578, ed, asp, Fe+	1975, fl	pl	355	-	50
49	multiple i.m.	284	R 689, L 463, ed, co, pneumo, Fe+	1523, fl	++, pl	110	11	450
50	multiple i.m.	401, hy	R 918, L 788, ed, co, Fe+	1882, co	++, pl	242	30	150

-, unremarkable, not present; ++, enlargement; R, right; L, left; ARDS, acute respiratory distress syndrome; asp, aspiration; cb, contraction bands; co, congestion; ed, edema; Fe+, iron-containing macrophages; fib, fibrosis; fl, fatty liver; hep, hepatitis; hy, hypertrophy; i.m., injection mark; mu, mushroom of blood-tingled foam; pl, portal lymph node; pneumo, bronchopneumonia; tracks, needle tracks.

The determination of the numerical density (n/mm^2) of astrocytes and microglia was performed at 400 × magnification with a counting grid *(4)*. For the quantification of microglia, the perivascular and parenchymal microglia was counted separately, then summed up as total microglia. The gray matter was analyzed following the "systematic row sampling," whereas the white matter, the hippocampal formation, the subcortical, and the brainstem regions were analyzed following the "random systematic sampling" *(4)*.

For the determination of ß-APP immunostaining, a semiquantitative scoring system was used with 0 being no ß-APP immunostaining; 1, moderate immunostaining, however focal; 2, scattered patches of ß-APP foci; and 3, extensive ß-APP deposits throughout large areas of the white matter.

For collagen type IV, the intensity of the immunostaining was evaluated using a 3-point rating scale. Staining reactivity was denoted as 1 for mild immunoreactivity, 2 for moderate immunoreactivity, and 3 for strong immunoreactivity. The numerical density of vessels for each staining intensity and the total numerical density of vessels was calculated by dividing the number of counted vessels by the total area of all measuring fields and expressed as n/mm^2.

The data were analyzed with the statistical program SPSS (Statistical Package for the Social Sciences, version 13.0 for Windows). The nonparametric Mann-Whitney U-test as well as the Spearman Rank correlation were used.

RESULTS

All drug deaths were polydrug abusers who died owing to acute drug intoxication (Table 2). Besides heroin in 30 cases, codeine/dihydrocodeine ($n = 10$), methadone ($n = 6$), cocaine ($n = 2$), and methylenedioxymethamphetamine ($n = 2$) could be detected as the major substance that caused death. Thus, 92% of all drug deaths were associated with the abuse of opioids. Concomitant use of other drugs and alcohol were frequently seen (Table 2). The major findings of the peripheral organs of the drug fatalities are listed in Table 3. None of the drug and control cases revealed signs of hepatic or pancreatic changes suggestive of long-term excessive alcohol abuse at general autopsy. None of the cases had a history of severe CNS trauma.

Neuropathological Investigations

The macroscopic data on brain weight, signs of brain edema, and increased intracranial pressure did not differ significantly between both groups. In none of the cases could significant herniation with secondary brain stem hemorrhages be detected.

The histopathological examination of the brains of controls and of polydrug abusers did not demonstrate changes due to infectious agents or cerebrovascular lesions. The amount and distribution of leptomeningeal fibrosis, congestion and cellular infiltrates as well as brain edema, vascular congestion, perivascular cuffing, perivascular hemorrhages, gliomesenchymal nodules, and any hypoxic nerve cell damage, as assessed in the routinely stained sections, did not statistically differ between both groups. There was no significant correlation between the measured parameters and postmortem interval. There was also no significant difference for the measured parameters between both sexes.

Neuronal Density

In the brains of polydrug abusers there was a significant nerve cell loss in the orbitofrontal, frontal, temporal, parietal and occipital cortex as well as in the caudate nucleus, putamen, globus pallidus, thalamus, substantia nigra, pons, inferior olivary nucleus, dentate nucleus, and the cerebellar granular cell layer as compared with controls. There was no significant difference between both groups for the neuronal number in the hippocampal formation and in the Purkinje cell layer of the cerebellum (Figs. 1 and 2).

White Matter Changes

On LFB staining, pallor of the white matter could be detected in six polydrug abuse cases and in one control case, but the difference was not statistically significant. However, in the white matter of all regions examined, ß-APP-immunoreactivity was significantly increased in the brains of polydrug abusers as compared to controls *(5)*.

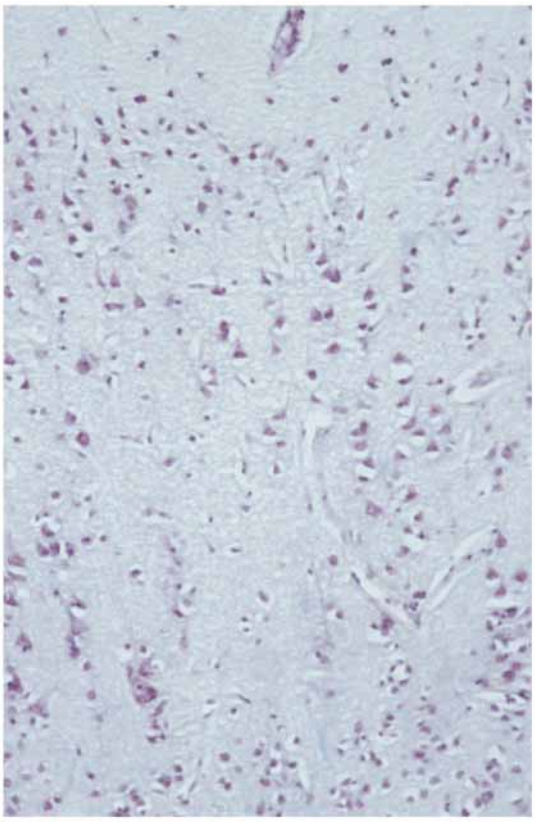

Fig. 1. Nerve cell loss within the occipital cortex of a drug abuser (Luxol-Fast-Blue stain, magnification ×100).

Astrocytes

In the brains of polydrug abusers, the numerical density of GFAP-positive astrocytes was significantly reduced in the gray and white matter in all regions examined, with the exception of the hippocampal CA1 region, the pyramidal tract and the cerebellar cortex (Fig. 3).

Microglia

In the brains of polydrug abusers, the numerical density of CR3/43-positive microglia (i.e., both perivascular and parenchymal) was significantly increased in the orbitofrontal, frontal, parietal, and occipital white matter as well as in the mesencephalon, pons, medulla oblongata, inferior olivary nucleus, and the cerebellum (Fig. 4). The numerical density of perivascular microglia was significantly increased only in the inferior olivary nucleus, whereas in the other brain regions there was no significant difference between both groups. In contrast, the numerical density of parenchymal microglia was significantly increased in the orbitofrontal, frontal, temporal, parietal and occipital white matter as well as in the mesencephalon, pons, medulla oblongata, inferior olivary nucleus, and the cerebellum.

Vascular System

The total extent and distribution of vascular congestion, perivascular cuffing, or perivascular hemosiderin deposits and hemorrhages did not statistically differ between both groups. However, in the brains of polydrug abusers the number of vessels showing hyalinotic thickening was significantly increased in the gray and white matter of the orbitofrontal, frontal, temporal, parietal, and occipital cortex as well as in the caudate nucleus, putamen, globus pallidus, internal capsule, and medulla oblongata (Fig. 5). The alterations consisted of concentric hyalinotic thickening, sometimes with luminal narrowing (Fig. 6A,B).

In the brains of polydrug abusers, the number of vessels showing endothelial proliferation was significantly increased in the gray and white matter of the orbitofrontal, frontal, temporal, parietal, and occipital cortex as well as in the caudate nucleus and substantia nigra (Fig. 7). The alterations consisted of a marked endothelial swelling and endothelial cell hyperplasia (Fig. 8A,B), but they never reached the extent of a true angiogenesis.

The results for the alterations of collagen type IV in the vascular basal lamina of the frontal, temporal, parietal, and occipital lobe have been reported previously *(6)*. Briefly, in the cortical gray and white matter of the brains of polydrug abusers, the number of vessels showing strong immunoreactivity for collagen type IV was significantly reduced, whereas the number of vessels with mild and moderate immunoreactivity was increased as compared to controls. The total numerical density of vessels was not significantly changed. In the other regions examined, similar changes could be observed in the caudate nucleus, mesencephalon, and medulla oblongata but not in the putamen, globus pallidus, internal capsule, thalamus, and pons (Fig. 9A,B).

DISCUSSION

Although animal and neuroimaging research within the past number of years have clarified various aspects of CNS alterations in the context of drug abuse, systematic morphological studies of the human brain have been lacking. Therefore, the aim of this study was a systematic morphological analysis of the brains of polydrug abusers. The major finding was a widespread neuronal loss, a reduction of GFAP-positive astrocytes, an axonal damage with concomitant microglia activation, as well as reactive and degenerative vascular changes.

Although this study was performed on a large well-documented group of polydrug deaths, some variables could not be excluded. The information about the duration and types of drug abused can only be estimated, since the first appearance of the individual in the police records does usually not reflect the actual beginning of drug abuse. Another problem consists of distinguishing between substance-specific effects related to the properties of the drug itself and secondary effects related to lifestyle (e.g., malnutrition, infections, and peripheral diseases).

The illicit substances taken by the polydrug abusers in our study reflect the characteristic spectrum that are consumed worldwide, with opioids being the major substances abused *(1,7)*. Because 92% of our polydrug deaths were associated

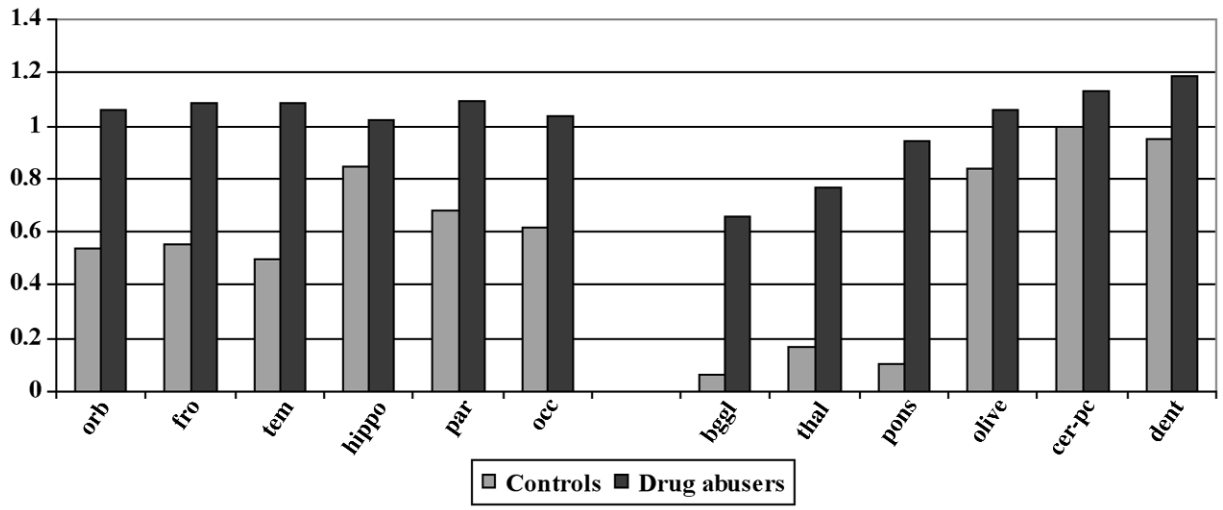

Fig. 2. Result of the semiquantitative scoring of nerve cell density demonstrating significantly higher score of nerve cell loss in the brains of drug abusers (for details and abbreviations *see* text).

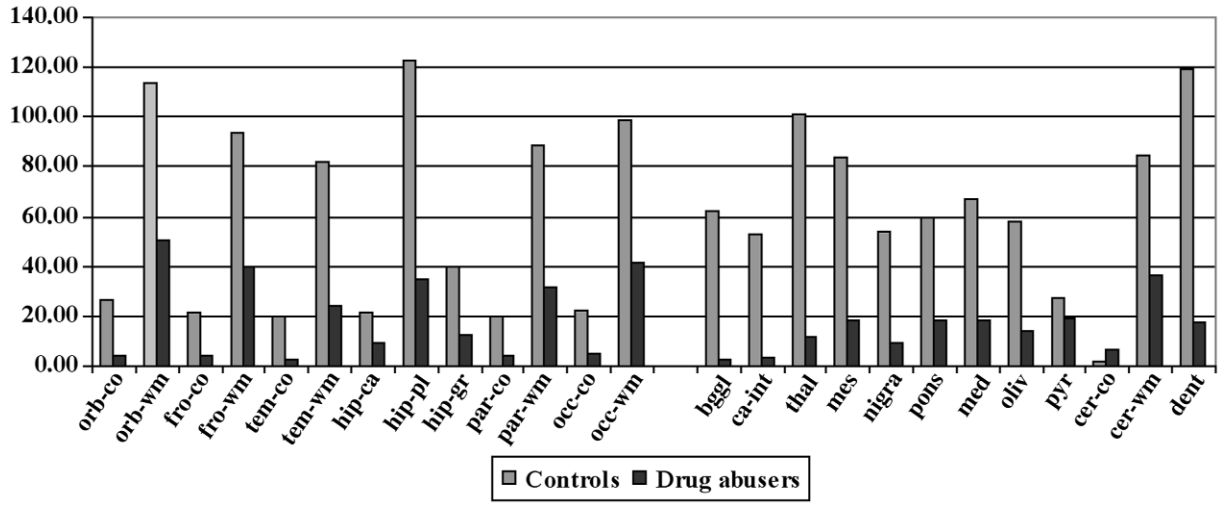

Fig. 3. Numerical density (n/mm^2) of GFAP-immunopositive astrocytes. There is a significant reduction of the number of GFAP-immunopositive astrocytes in the brains of drug abusers as compared to controls (for abbreviations *see* text).

with long-standing opioid abuse, the observed alterations are most probably owing to these substances. Because all subtypes of opiate receptors are expressed on neurons, astrocytes, microglia, and endothelial cells *(8,9)*, opioids exert their influence on almost all cell types of the CNS.

There are only few reports on histopathological alterations in the brain of drug abusers, predominantly describing edema, vascular congestion, ischemic nerve cell damage, and neuronal loss *(7,10–12)*. These changes have been attributed to toxic primary respiratory failure and are therefore considered as being nonspecific *(7)*. However, in most of these studies, there was no statistical comparison to a control group and systematic data on frequency or topography of the lesions are lacking.

In this study, the findings mentioned above could be confirmed only partially. In polydrug abusers hypoxic nerve cell damage was significantly more often present only in the orbitofrontal, temporal, and occipital cortex. In contrast, there was a widespread neuronal loss in the brains of polydrug abusers, with the exception of the hippocampal formation and the Purkinje cell layer. In both regions there was also no significant reduction of GFAP-positive astrocytes.

In addition, there were concomitant vascular alterations in the cortical regions and a reduction of GFAP-positive astrocytes, but no surrounding microglial activation. Within the subcortical regions there was a significant neuronal loss and a reduction of GFAP-positive astrocytes, but only scarce vascular alterations. Therefore, a vascular mechanism of the neu-

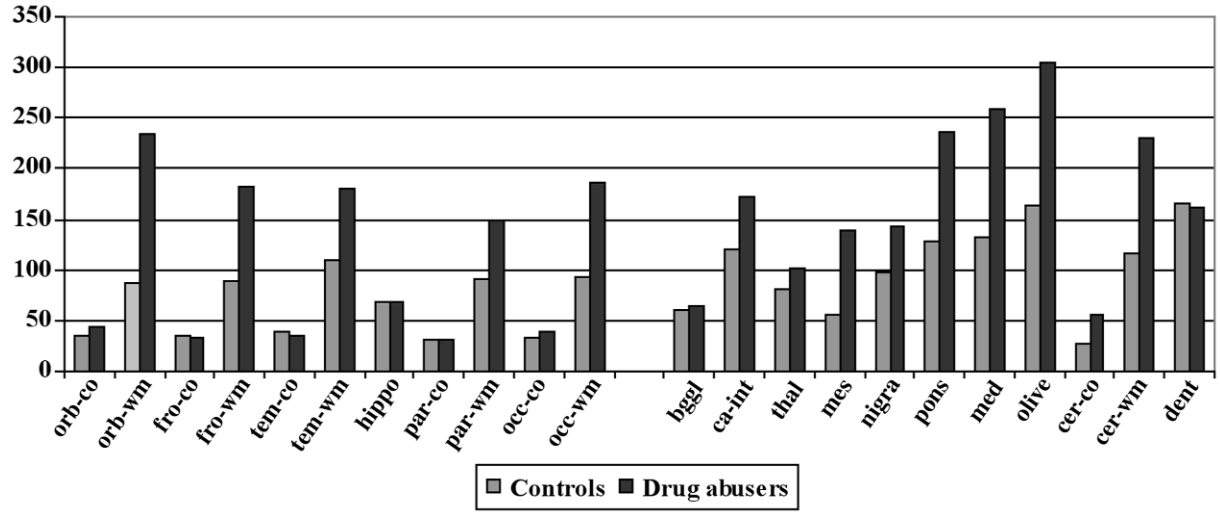

Fig. 4. Numerical density (n/mm^2) of parenchymal and perivascular CR3/43-immunopositive microglia in the brains of drug abusers as compared to controls (for abbreviations *see* text).

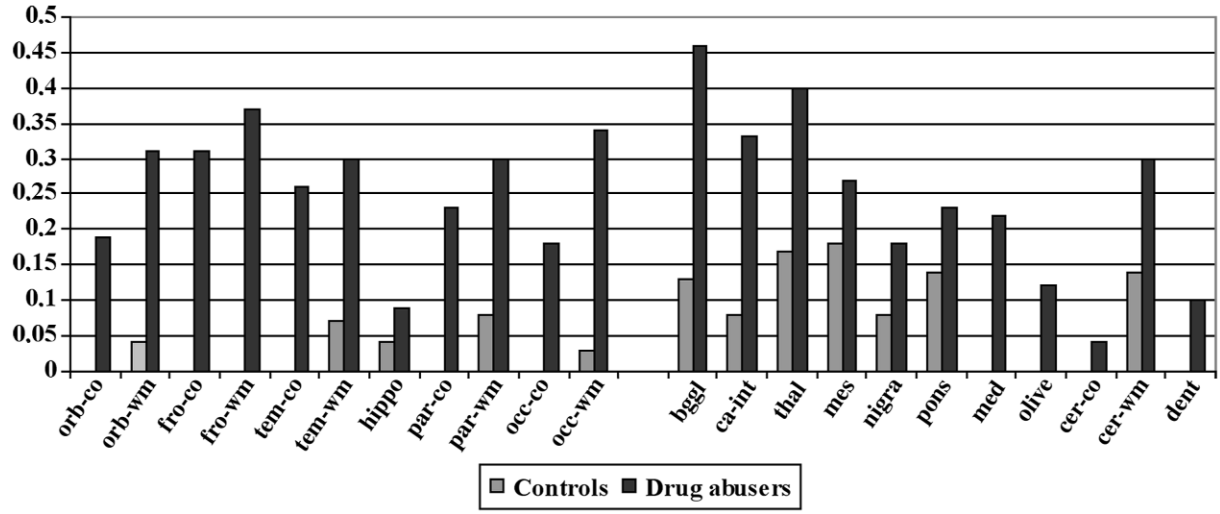

Fig. 5. Result of the semiquantitative scoring of vascular thickening demonstrating significantly higher score in the brains of drug abusers (for details and abbreviations *see* text).

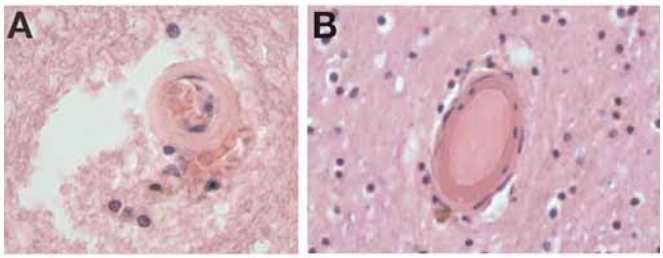

Fig. 6. Hyalinotic vascular thickening in the brains of drug abusers: **(A)** parietal, **(B)** temporal (H&E stain, magnification ×200).

ronal loss cannot be assumed. An age-associated neuronal reduction can also be excluded because the mean age of the control group was higher than that of the polydrug abusers.

Although the neuronal loss could be induced by recurrent hypoxic–ischemic episodes owing to respiratory depression during the intoxicated state, the reduction of GFAP-positive astrocytes argues against such a phenomenon as the sole cause. Furthermore, CNS lesions after global hypoxic–ischemic damage are predominantly seen in the Purkinje cell layer of the cerebellum and the hippocampal formation *(13)*. Because the nerve cell density in these regions was not significantly changed between both groups, other factors must be of pathogenetic significance.

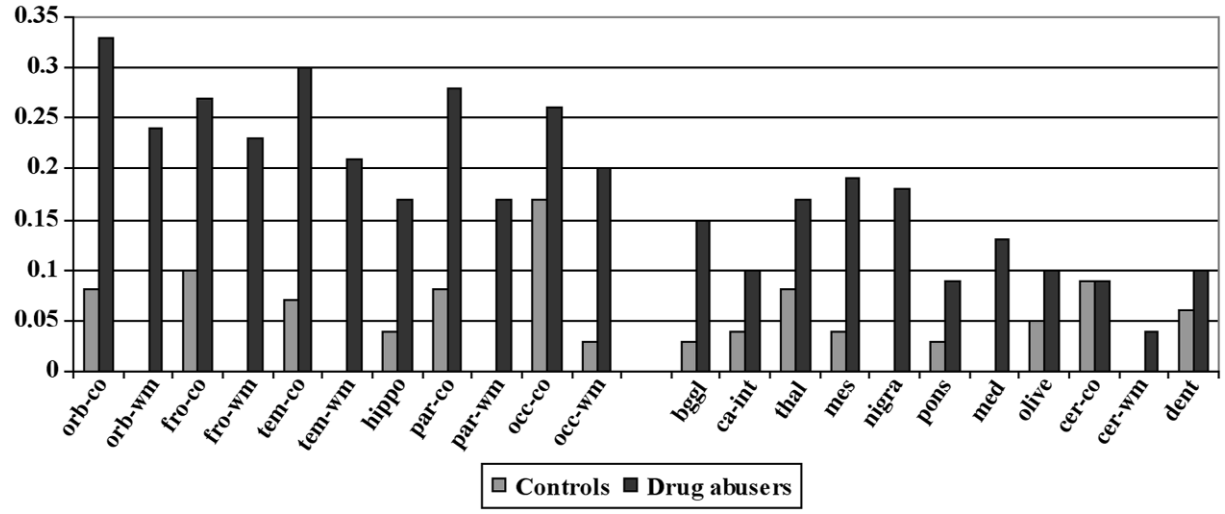

Fig. 7. Result of the semiquantitative scoring of endothelial proliferation demonstrating significantly higher score in the brains of drug abusers (for details and abbreviations *see* text).

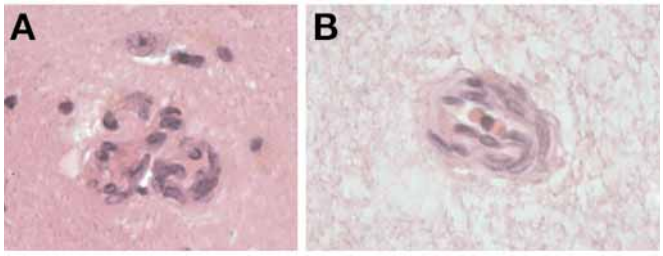

Fig. 8. Endothelial proliferation in the brain of drug abusers: **(A)** caudate nucleus, **(B)** occipital (H&E stain, magnification ×200).

Besides hypoxic–ischemic nerve cell damage, apoptotic processes can result in neuronal cell death *(14)*. It has been shown for nearly all drugs of abuse that apoptosis can occur *(15–21)*. In these studies it was shown that drugs of abuse can induce neuronal apoptosis by an increased expression of pro-apoptotic factors (e.g., p53, bax, caspases, endonucleases) and by a decreased expression of the anti-apoptotic oncoprotein bcl-2. Furthermore, a drug-induced decrease of the astrocytic glutamate transporter resulted in an increase of extracellular glutamate with subsequent excitatory nerve cell damage *(22)*. However, data on the human brain are lacking so far. Another possibility for the neuronal loss might be drug-induced alterations of neurofilament (NF) proteins *(23)*. In opioid deaths, a marked reduction in total NF proteins, immunoreactive NF proteins, and an aberrant hyperphosphorylation of NF has been demonstrated *(24,25)*.

White Matter

Although there were no significant white matter changes seen on myelin-stained sections, our results show a widespread axonal damage in the brains of polydrug abusers. Because this group did not significantly differ from the controls in the presence of brain edema or signs of increased intracranial pressure, the mechanism of a secondary phenomenon owing to global hypoxia–ischemia cannot explain our findings. Furthermore, the microglial activation selectively in the white matter of polydrug abusers argues against an acute or agonal phenomenon and is indicative of a long-standing progressive process.

Based on these findings, it seems likely that drugs of abuse might induce direct toxic–metabolic axonal damage, which might be induced or enhanced by cerebral hypoxia. Besides these direct mechanisms, the activated microglia could increase the axonal damage by the release of cytotoxic substances. The extent of the axonal damage is likely to be underestimated, because ß-APP only detects relatively recently damaged axons *(26)*, whereas the duration of the abuse of drugs often lasts several years. Therefore, in conjunction with the microglial activation, a chronic-progressive process has to be considered, which might be initiated and supported by drugs of abuse. The alterations might be the morphological correlate of the observed demyelination and hyperintense areas seen on magnetic resonance imaging *(2,27,28)*.

Astrocytes

Although an increased expression of GFAP in astrocytes (astrogliosis) has been described in various CNS lesions *(29)*, there are only few data on toxic CNS damage (*30*). In an older study, widespread fragmentation and a numerical depletion of astrocytes in the white matter have been reported in the brains of drug deaths *(12)*. In HIV-positive drug abusers, HIV-negative drug abusers, and non-drug-using controls there was no statistical difference between the three groups in relation to astrocytes *(31,32)*. In the prefrontal cortex of opioid deaths, the immunodensity of GFAP was found unchanged *(24)*. Morphine inhibited astrocytic proliferation in murine cell cultures, and there was a dysregulation of calcium homeostasis and an increase of reactive oxygen species *(33)*. After cocaine

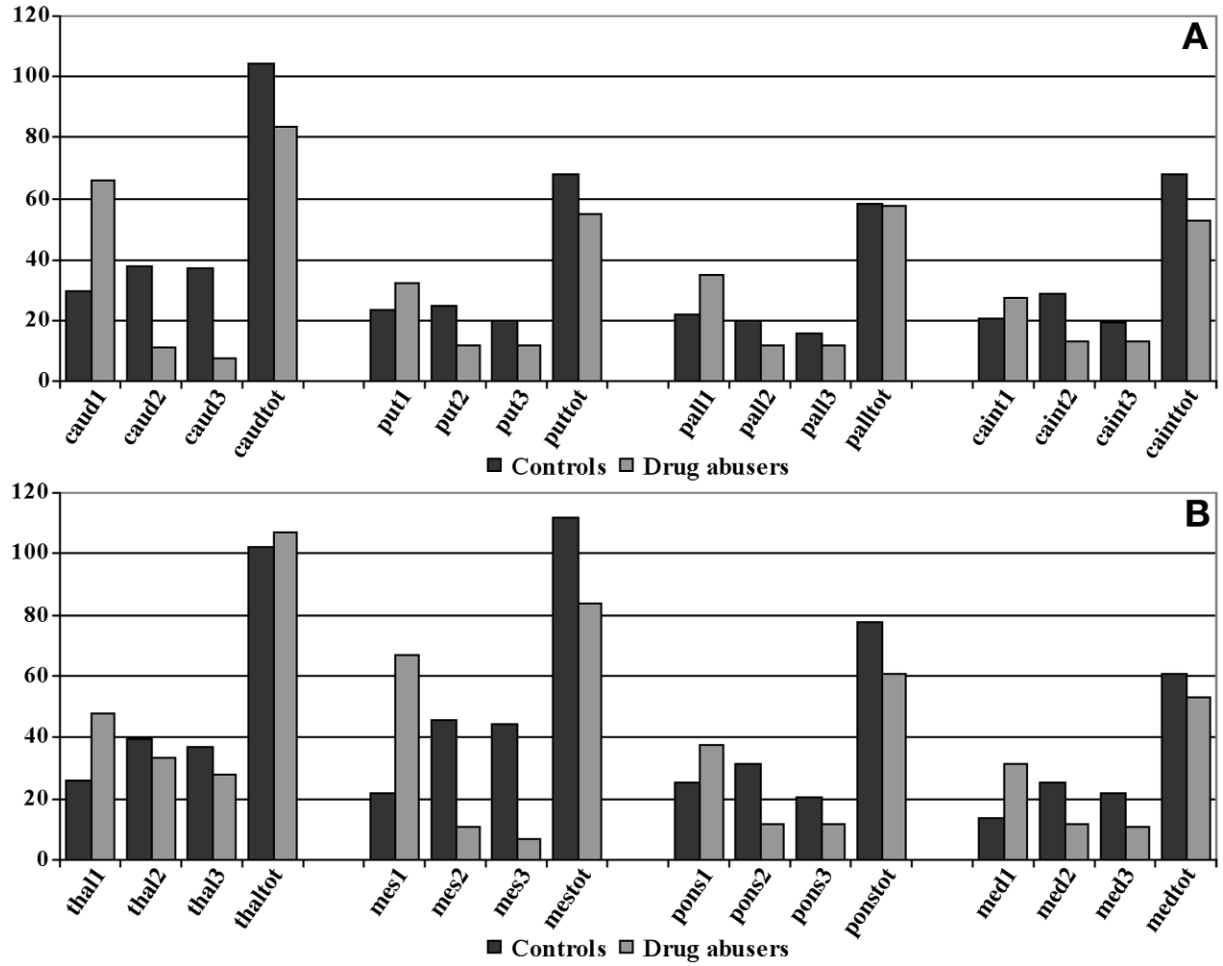

Fig. 9. **(A)** Numerical density (n/mm^2) of blood vessels in the basal ganglia according to the staining intensity for collagen type IV in drug abusers as compared to controls. **(B)** Numerical density (n/mm^2) of blood vessels in the subcortical regions according to the staining intensity for collagen type IV in drug abusers as compared to controls (for abbreviations *see* text).

administration, modifications in astrocytic numbers, cell size, and shape complexity were seen *(34)*.

The reduction of GFAP-positive astrocytes suggests drug-induced cell damage. One possible mechanism could be the interference of drugs with the GFAP-gene transcription inducing an altered GFAP-phosphorylation *(35)*. Furthermore, the induction of a cytochrome P450 isoform by drugs of abuse with the generation of free radicals *(36)* and subsequent damage of astrocytes might be conceivable. In addition, a drug-mediated effect on the astrocytic cytoskeleton, similar to the neuronal neurofilament proteins *(23-25)* might contribute to the decrease of GFAP-immunoreactivity.

I2-imidazoline receptors are involved in the regulation of the GFAP expression *(23)*. In the frontal cortex of heroin deaths the density of I2-imidazoline receptors and the immunoreactivity of the related imidazoline receptor protein were decreased *(37)*. Therefore, a downregulation of I2-imidazoline receptors in astrocytes could be associated with our observation and might represent a specific long-term effect of drugs of abuse on astrocytes.

Because astrocytes are of eminent importance for the maintenance of the blood–brain barrier (BBB) integrity *(38)* our findings might also be indicative of an indirect impairment of the BBB. Because GFAP expression is also essential for normal white matter architecture *(39)*, its reduction might contribute to the white matter changes seen in polydrug deaths.

Microglia

The activation of microglia predominantly in the white matter of polydrug abusers is in accordance with the findings of other authors *(10,11,32)*. As mentioned earlier, this activation is most probably induced by the axonal damage and not the result of a direct drug-associated effect. The activation of microglia might lead to the release of cytotoxic substances and a disruption of synaptic integrity.

Cerebral Microvasculature

Cerebrovascular accidents are frequently seen in the context of drug abuse, but to date there is no consensus about the cause *(1,2)*. As one possible pathogenetic mechanism, a drug-induced vasculitis has been postulated *(40)*. However, in our study, vasculitic changes could not be observed, so that we cannot confirm the regular occurence of a vasculitis in drug abusers.

In a study of AIDS patients, small-vessel thickening, perivascular space dilatation, pigment deposition, vessel wall mineralization, and perivascular inflammatory cell infiltrates were seen in 50% of then former drug abusers *(41)*.

It has been shown that cocaine enhances the expression of inflammatory cytokines, adhesion molecules, and chemokines on brain endothelial cells with consequent increase in permeability of the BBB *(42,43)*. After chronic cocaine administration, thrombosis, endothelial thickening, vascular wall fibrosis, and rupture of the basement membrane of brain capillaries have been observed in rats *(44)*. Methamphetamine induced disturbances in cellular redox status and upregulation of inflammatory genes in brain endothelial cells *(45)*.

On neuroimaging, small areas of demyelination, focal perfusion deficits, a reduction of the cerebral glucose metabolism, and hyperintense areas have been described in the brains of drug abusers *(3,27,28,46,47),* but to date there is no consensus about the cause or possible morphological substrates. Our study demonstrated profound alterations in the cerebral microvasculature. There was reactive endothelial cell proliferation, degenerative hyalinotic thickening, and a decrease of the collagen type IV content of the vascular basal lamina. A degeneration of the vascular basal lamina can result in an increased permeability and a reduced electrical resistance of the BBB *(48)*. Therefore, this noninflammatory vasculopathy can be considered as the morphological substrate of a disturbed BBB and might be associated with the alterations seen on neuroimaging.

In conclusion, our findings demonstrate that drugs of abuse initiate a cascade of interacting toxic, vascular and hypoxic factors which finally result in widespread disturbances within the complex network of CNS cell–cell interactions.

Educational Message

1. Widespread alterations can be detected in the brains of drug abusers using histology, immunohistochemistry, and morphometry.
2. There is a significant nerve cell loss in nearly all brain regions.
3. The numerical density of GFAP-positive astrocytes is reduced in the gray and white matter.
4. The numerical density of CR3/43-positive microglia is increased in the white matter as well as in the brainstem, inferior olivary nucleus, and the cerebellum.
5. There is a reactive endothelial cell proliferation, degenerative hyalinotic thickening, and a loss of immunoreactivity for collagen type IV within the vascular basal lamina.

ACKNOWLEDGMENTS

The authors are grateful to Susanne Ring and Miriam Finelli for their excellent technical assistance. The authors thank Dr. Ida C. Llenos for correcting the manuscript. The authors thank Veronika Paetzold, Florence Payrhammer, Katharina Rohrmoser, and Claus Kroehling for performing some of the investigations. This study has been supported by the Friedrich-Baur-Stiftung of the Medical Faculty of the Ludwig-Maximilians-University Munich (Grant No.: 0017/2000).

The authors have stated that they do not have a significant financial interest or other relationship with any product manufacturer or provider of services discussed in this article.

REFERENCES

1 Büttner A, Weis S. Central nervous system alterations in drug abuse. In: Tsokos M, ed. Forensic Pathology Reviews, Vol. 1. Totowa, NJ: Humana Press, 2004, pp. 79–136.
2 Karch SB. Karch's Pathology of Drug Abuse. 3rd ed., Boca Raton: CRC Press, 2002.
3 Kaufman M.J. Brain Imaging in Substance Abuse: Research, Clinical, and Forensic Applications. Totowa, NJ: Humana Press, 2001.
4 Weis S. Morphometry in the neurosciences. In: Wenger E, Dimitov L, eds. Digital Image Processing and Computer Graphics. Theory and Applications. München: Oldenburg Verlag, 1991, pp. 306–326.
5 Büttner A, Rohrmoser K., Mall G, Penning R, Weis S. Widespread axonal damage in the brain of drug abusers as evidenced by accumulation of ß-amyloid precursor protein (ß-APP): An immunohistochemical investigation. Addiction in press.
6 Büttner A, Kroehling C, Mall G, Penning R, Weis S. Alterations of the vascular basal lamina in the cerebral cortex in drug abuse: A combined morphometric and immunohistochemical investigation. Drug Alc Dep 2005;69:63–70.
7 Oehmichen M, Meiner C, Reiter A, Birkholz M. Neuropathology in non-human immunodeficiency virus-infected drug addicts: hypoxic brain damage after chronic intravenous drug abuse. Acta Neuropathol 1996;91:642–646.
8 Mansour A, Khachaturian H, Lewis ME, Akil H, Watson SJ. Anatomy of CNS opioid receptors. Trends Neurosci 1988;11: 308–314.
9 Stefano GB, Hartman A, Bilfinger TV, et al. Presence of the μ_3 opiate receptor in endothelial cells. Coupling to nitric oxide production and vasodilation. J Biol Chem 1995;270:30,290–30,293.
10 Gosztonyi G, Schmidt V, Nickel R, et al. Neuropathologic analysis of postmortal brain samples of HIV-seropositive and -seronegative i.v. drug addicts. Forensic Sci Int 1993;62:101–105.
11 Makrigeorgi-Butera M, Hagel C, Laas R, Püschel K, Stavrou D. Comparative brain pathology of HIV-seronegative and HIV-infected drug addicts. Clin Neuropathol 1996;15:324–329.
12 Pearson J, Richter RW. Addiction to opiates: neurologic aspects. In: Vinken PJ, Bruyn GW, eds. Handbook of Clinical Neurology. Intoxications of the Nervous System, Part II. Amsterdam: North-Holland, 1979, pp. 365–400.
13 Hart MN, Galloway GM, Dunn MJ. Perivascular anoxia–ischemia lesions in the human brain. Neurology 1975;25:477–482.
14 Yuan J, Yankner BA. Apoptosis in the nervous system. Nature 2000;407:802–809.

15 Boronat MA, García-Fuster MJ, García-Sevilla JA. Chronic morphine induces up-regulation of the pro-apoptotic Fas receptor and down-regulation of the anti-apoptotic Bcl-2 oncoprotein in rat brain. Br J Pharmacol 2001;134:1263–1270.
16 Campbell VA. Tetrahydrocannabinol-induced apoptosis of cultured cortical neurones is associated with cytochrome c release and caspase-3 activation. Neuropharmacology 2001;40: 702–709.
17 Davidson C, Gow AJ, Lee TH, Ellinwood EH. Methamphetamine neurotoxicity: necrotic and apoptotic mechanisms and relevance to human abuse and treatment. Brain Res Rev 2001;36:1–22.
18 Hu S, Sheng WS, Lokensgard JR, Peterson PK. Morphine induces apoptosis of human microglia and neurons. Neuropharmacology 2002;42:829–836.
19 Jiang Y, Yang W, Zhou Y, Ma L. Up-regulation of murine double minute clone 2 (MDM2) gene expression in rat brain after morphine, heroin, and cocaine administrations. Neurosci Lett 2003;352:216–220.
20 Mao J, Sung M, Ji RR, Lim G. Neuronal apoptosis associated with morphine tolerance: evidence for an opioid-induced neurotoxic mechanism. J Neurosci 2002;22:7650–7661.
21 Stumm G, Schlegel J, Schäfer T, et al. Amphetamines induce apoptosis and regulation of bcl-x splice variants in neocortical neurons. FASEB J 1999;13:1065–1072.
22 Thorlin T, Roginski RS, Choudhury K, et al. Regulation of the glial glutamate transporter GLT-1 by glutamate and δ-opioid receptor stimulation. FEBS Lett 1998;425:453–459.
23 Boronat MA, Olmos G, García-Sevilla JA. Attenuation of tolerance to opioid-induced antinociception and protection against morphine-induced decrease of neurofilament proteins by idazoxan and other I_2-imidazoline ligands. Br J Pharmacol 1998;125:175–185.
24 Ferrer-Alcón M, García-Sevilla JA, Jaquet PE, et al. Regulation of nonphosphorylated and phosphorylated forms of neurofilament proteins in the prefrontal cortex of human opioid addicts. J Neurosci Res 2000;61:338–349.
25 García-Sevilla JA, Ventayol P, Busquets X, La Harpe R, Walzer C, Guimón J. Marked decrease of immunolabelled 68 kDa neurofilament (NF-L) proteins in brains of opiate addicts. Neuroreport 1997;8:1561–1570.
26 Medana IM, Esiri MM. Axonal damage: a key predictor of outcome in human CNS diseases. Brain 2003;126:515–530.
27 Ernst M, London ED. Brain imaging studies of drug abuse: therapeutic implications. Semin Neurosci 1997;9:120–130.
28 Volkow ND, Valentine A, Kulkarni M. Radiological and neurological changes in the drug abuse patient. A study with MRI. J Neuroradiol 1988;15:288–293.
29 Chen Y, Swanson RA. Astrocytes and brain injury. J Cereb Blood Flow Metab 2003;23:137–149.
30 O'Callaghan JP. Quantitative features of reactive gliosis following toxicant-induced damage of the CNS. Ann NY Acad Sci 1993;679:195–210.
31 Anderson CE, Tomlinson GS, Pauly B, et al. Relationship of Nef-positive and GFAP-reactive astrocytes to drug use in early and late HIV infection. Neuropathol Appl Neurobiol 2003;29: 378–388.
32 Tomlinson GS, Simmonds P, Busuttil A, Chiswick A, Bell JE. Upregulation of microglia in drug users with and without presymptomatic HIV infection. Neuropathol Appl Neurobiol 1999;25:369–379.
33 Hauser KF, Harris-White ME, Jackson JA, Opanashuk LA, Carney JM. Opioids disrupt Ca^{2+} homeostasis and induce carbonyl oxyradical production in mouse astrocytes in vitro: transient increases and adaptation to sustained exposure. Exp Neurol 1998;151:70–76.
34 Fattore L, Puddu MC, Picciau S, et al. Astroglial in vivo response to cocaine in mouse dentate gyrus: a quantitative and qualitative analysis by confocal microscopy. Neuroscience 2002; 110:1–6.
35 Stadlin A, Lau JWS, Szeto YK. A selective regional response of cultured astrocytes to methamphetamine. Ann NY Acad Sci 1998;844:108–121.
36 Castagnoli N Jr, Castagnoli KP. Metabolic bioactivation reactions potentially related to drug toxicities. NIDA Res Monogr 1997;173:85–105.
37 Sastre M, Ventayol P, García-Sevilla JA. Decreased density of I_2-imidazoline receptors in the postmortem brains of heroin addicts. Neuroreport 1996;7:509–512.
38 Abbott NJ. Astrocyte-endothelial interactions and blood–brain barrier permeability. J Anat 2002;200:629–638.
39 Liedtke W, Edelmann W, Bieri PL, et al. GFAP is necessary for the integrity of white matter architecture and long-term maintenance myelination. Neuron 1996;17:607–615.
40 Brust JCM. Vasculitis owing to substance abuse. Neurol Clin 1997;15:945–957.
41 Connor MD, Lammie GA, Bell JE, Warlow CP, Simmonds P, Brettle RP. Cerebral infarction in adult AIDS patients: observations from the Edinburgh HIV autopsy cohort. Stroke 2000;31:2117–2126.
42 Gan X, Zhang L, Berger O, et al. Cocaine enhances brain endothelial adhesion molecules and leukocyte migration. Clin Immunol 1999;91:68–76.
43 Lee YW, Hennig B, Fiala M, Kim KS, Toborek M. Cocaine activates redox-regulated transcription factors and induces TNF-α expression in human brain endothelial cells. Brain Res 2001;920:125–133.
44 Barroso-Moguel R, Villeda-Hernández J, Méndez-Armenta M, Ríos C. Brain capillary lesions produced by cocaine in rats. Toxicol Lett 1997;92:9–14.
45 Lee YW, Hennig B, Yao J, Toborek M. Methamphetamine induces AP-1 and NF-kappaB binding and transactivation in human brain endothelial cells. J Neurosci Res 2001;66: 583–591.
46 Christensen JD, Kaufman MJ, Levin JM, et al. Abnormal cerebral metabolism in polydrug abusers during early withdrawal: a ^{31}P MR spectroscopy study. MRM 1996;35:658–663.
47 Stapleton JM, Morgan MJ, Phillips RL, et al. Cerebral glucose utilization in polysubstance abuse. Neuropsychopharmacology 1995;13:21–31.
48 Tilling T, Engelbertz C, Decker S, Korte D, Hüwel S, Galla HJ. Expression and adhesive properties of basement membrane proteins in cerebral capillary endothelial cell cultures. Cell Tissue Res 2002;310:19–29.